ARTICLE

BIOTECHNOLOGY and BIOENGINEERING

NADPH-Dependent Reductive Biotransformation With *Escherichia coli* and Its *pfkA* Deletion Mutant: Influence on Global Gene Expression and Role of Oxygen Supply

Solvej Siedler, Stephanie Bringer, Tino Polen, Michael Bott

Institut für Bio- und Geowissenschaften, IBG-1: Biotechnologie, Forschungszentrum Jülich D-52425, Jülich, Germany; telephone: +49-2461-61-3476; fax: +49-2461-61-2710; e-mail: st.bringer-meyer@fz-juelich.de; telephone: +49-2461-61-3294; fax: +49-2461-61-2710; e-mail: m.bott@fz-juelich.de

ABSTRACT: An *Escherichia coli* Δ*pfkA* mutant lacking the major phosphofructokinase possesses a partially cyclized pentose phosphate pathway leading to an increased NADPH per glucose ratio. This effect decreases the amount of glucose required for NADPH regeneration in reductive biotransformations, such as the conversion of methyl acetoacetate (MAA) to (*R*)-methyl 3-hydroxybutyrate (MHB) by an alcohol dehydrogenase from *Lactobacillus brevis*. Here, global transcriptional analyses were performed to study regulatory responses during reductive biotransformation. DNA microarray analysis revealed amongst other things increased expression of *soxS*, supporting previous results indicating that a high NADPH demand contributes to the activation of SoxR, the transcriptional activator of *soxS*. Furthermore, several target genes of the ArcAB two-component system showed a lower mRNA level in the reference strain than in the Δ*pfkA* mutant, pointing to an increased QH_2/Q ratio in the reference strain. This prompted us to analyze yields and productivities of MAA reduction to MHB under different oxygen regimes in a bioreactor. Under anaerobic conditions, the specific MHB production rates of both strains were comparable ($7.4 \pm 0.2\ mmol_{MHB}\ h^{-1}\ g_{cdw}^{-1}$) and lower than under conditions of 15% dissolved oxygen, where those of the reference strain ($12.8\ mmol\ h^{-1}\ g_{cdw}^{-1}$) and of the Δ*pfkA* mutant ($11.0\ mmol\ h^{-1}\ g_{cdw}^{-1}$) were 73% and 49% higher. While the oxygen transfer rate (OTR) of the reference strain increased after the addition of MAA, presumably due to the oxidation of the acetate accumulated before MAA addition, the OTR of the Δ*pfkA* strain strongly decreased, indicating a very low respiration rate despite sufficient oxygen supply. The latter effect can likely be attributed to a restricted conversion of NADPH into NADH via the soluble transhydrogenase SthA, as the enzyme is outcompeted in the presence of MAA by the recombinant NADPH-dependent alcohol dehydrogenase. The differences in respiration rates can explain the suggested higher ArcAB activity in the reference strain.

Biotechnol. Bioeng. 2014;9999: 1–9.

KEYWORDS: *Escherichia coli*; resting cells; phosphofructokinase; SthA transhydrogenase; DNA microarrays; reductive whole-cell biotransformation

Introduction

Microbial whole-cell biotransformation is implemented in industry for the production of chiral alcohols (Ishige et al., 2005). A variety of dehydrogenases catalyze the enantio- and regioselective reduction of ketones and depend on nicotinamide adenine dinucleotide coenzymes (NADH or NADPH) for hydride transfer (Goldberg et al., 2007). Efficient coenzyme recycling by engineered strains transforming the oxidized coenzyme back to its reduced form is essential for efficient reductive whole-cell biotransformations and different possibilities for catching reducing power have been reported (Goldberg et al., 2007).

Recently, glucose was used as the electron donor for cofactor regeneration under anaerobic as well as aerobic conditions using metabolically engineered *Escherichia coli* strains (Akinterinwa and Cirino, 2011; Chin and Cirino, 2011; Siedler et al., 2011, 2012). In Figure S1, the reactions yielding NADH or NADPH during aerobic catabolism of glucose are shown. Partial cyclization of the pentose phosphate pathway (PPP) by deletion of the phosphofructokinase genes (*pfkA*, *pfkB*) resulted in an increased NADPH per glucose ratio and in an improved product-to-glucose yield of the NADPH-dependent biotransformation of the β-keto ester methyl acetoacetate (MAA) to the chiral hydroxy ester (*R*)-methyl 3-hydroxybutyrate (MHB), which is catalyzed by

Correspondence to: S. Bringer and M. Bott

Contract grant sponsor: Ministry of Innovation, Science, Research and Technology of North Rhine-Westphalia (Bio.NRW, Technology Platform Biocatalysis, RedoxCell)
Contract grant number: W0805wb001b
Received 4 November 2013; Revision received 25 February 2014; Accepted 14 April 2014
Accepted manuscript online xx Month 2014;
Article first published online in Wiley Online Library (wileyonlinelibrary.com).
DOI 10.1002/bit.25271

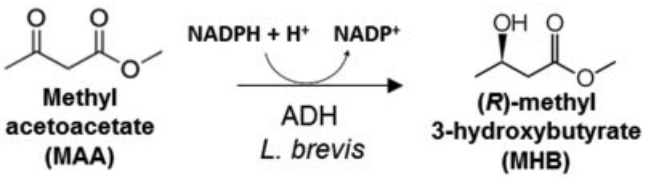

Figure 1. NADPH-dependent reduction of methyl acetoacetate catalyzed by an alcohol dehydrogenase from *Lactobacillus brevis*, which was used as a model reaction for reductive biotransformation in this study.

an alcohol dehydrogenase from *Lactobacillus brevis* (Fig. 1) (Siedler et al., 2011). The partially cyclized PPP was confirmed by ^{13}C metabolic flux analysis, which revealed a positive net flux from fructose 6-phosphate to glucose 6-phosphate in the *E. coli* Δ*pfkA* mutant (Siedler et al., 2012). Moreover, the carbon flux through the lower part of the Embden-Meyerhof pathway (EMP) and through the tricarboxylic acid (TCA) cycle was reduced in the Δ*pfkA* mutant to one-fourth of that of the reference strain (Siedler et al., 2012). *E. coli* possesses two pyridine nucleotide transhydrogenases to adjust the relative concentrations of NADPH and NADH, the cytoplasmic enzyme SthA (previously termed UdhA) and the membrane-bound enzyme PntAB (Jackson, 2003). While PntAB drives NADPH generation from NADH by using the proton motive force, SthA catalyzes the reduction of NAD^+ by NADPH (Sauer et al., 2004). In the ^{13}C metabolic flux analysis mentioned above, a significantly higher flux through the SthA-catalyzed reaction was observed during growth of the Δ*pfkA* mutant, pointing to an important role of SthA in this mutant (Siedler et al., 2012).

In this work, we analyzed the influence of reductive biotransformation on global gene expression by DNA microarrays. As in our previous studies, we used *E. coli* BL21(DE3) or its Δ*pfkA* mutant, both expressing the *L. brevis* ADH, and the NADPH-dependent reduction of MAA to MHB as the model reaction. The results obtained in the transcriptome studies prompted us to perform whole-cell biotransformation experiments under controlled conditions of oxygen availability. In the course of these studies, the role of the soluble transhydrogenase (SthA) was unraveled, as well as potential bottlenecks in the reference strain and its Δ*pfkA* mutant.

Materials and Methods

Bacterial Strains and Plasmids, Media and Growth Conditions

Strains and plasmids used in this work are listed in Table I. The Δ*pfkA* mutant strain was constructed as described previously (Siedler et al., 2011). *E. coli* strains were transformed by the method described by Hanahan et al. (1991) and cultivated in 2xYT medium (16 g L^{-1} tryptone, 10 g L^{-1} yeast extract, 5 g L^{-1} sodium chloride). The media contained 100 μg mL^{-1} ampicillin to maintain plasmid pBtac-*Lbadh*.

Whole-Cell Biotransformation

For the cultivation of the recombinant *E. coli* Star BL21(DE3) strain and its Δ*pfkA* derivative, both carrying the plasmid pBtac-*Lbadh*, a single colony of each strain was inoculated into 20 mL of 2xYT medium containing 100 μg mL^{-1} ampicillin and grown overnight at 37°C and 140 rpm. These pre-cultures were used to inoculate the main cultures to an OD_{600} of 0.05. The main cultures were grown in 600 mL of 2xYT medium containing 100 μg mL^{-1} ampicillin at 37°C and 130 rpm to an OD_{600} of 0.3, then *Lbadh* expression was induced with 1 mM of IPTG and the cultures incubated for another 3 h at 37°C and 130 rpm. The cells with an OD_{600} between 2 and 4.5, which had been determined as the optimal cell density for subsequent whole-cell biotransformation, were then harvested by centrifugation (4,000*g*, 7 min) and resuspended in 190 mL reaction buffer containing 111 mM (2% w/v) glucose, 2 mM $MgSO_4$, and 250 mM potassium phosphate buffer, pH 6.5, to a cell density of 3 g cell dry weight (cdw) per liter. Biotransformations were performed at 37°C in a bioreactor system (Dasgip, Jülich, Germany) composed of four 400-mL vessels, each equipped with electrodes for measuring the dissolved oxygen concentration (DO) and the pH. The system enabled these two parameters to be kept constant. The carbon dioxide concentration in the exhaust gas was measured continuously by an infrared spectrometer and the oxygen concentration by a zirconium dioxide sensor. The oxygen availability was kept constant at 15% DO by mixing air, O_2 and N_2. Calibration was performed by gassing with air (100% DO) and N_2 (0% DO). Anaerobic conditions were provided by gassing with 100% N_2.

Table I. Strains and plasmids used in this work.

Strains/plasmids	Relevant characteristics	Refs.
Strains		
Escherichia coli BL21(DE3) Star	F^- *ompT* $hsdS_B(r_B^-, m_B^-)$ *gal dcm rne*131 (DE3)	Invitrogen
Reference strain	*E. coli* BL21(DE3) Star with pBtac*Lbadh*	Siedler et al. (2011)
Δ*pfkA*	*E. coli* BL21(DE3) Star Δ*pfkA* with pBtac*Lbadh*	Siedler et al. (2011)
Plasmids		
pBTac-*Lbadh*	Amp^R, P_{tac}, pBR322 ori; expression vector for *E. coli* with *adh* gene from *Lactobacillus brevis*	X-Zyme, Ernst et al. (2005)

The agitation speed was kept constant at 900 rpm. Controlling and recording of all data as well as calculation of oxygen transfer rates (OTR) and CO_2 transfer rates (CTR) was carried out by the "Fedbatch Pro" software (Dasgip, Jülich, Germany).

The biotransformation was started by adding 60 mM MAA dissolved in water and pre-warmed to 37°C after the OTR had become constant. The increase of the OTR signal in the first 20 min was caused by the slow increase of the dissolved oxygen in the media, due to device-specific parameters. For the conversion of MAA to MHB, it was shown that there is no substrate or product inhibition, and neither the substrate nor the product is toxic to the cells under the chosen conditions up to 100 mM (Tan, 2006). Specific productivities (mmol MHB per hour per gram cdw) were determined by taking samples at 15-min time intervals over a period of 2 h. MHB and glucose concentrations of the samples were determined (see below). Specific productivities were calculated by dividing the slopes of graphs showing MHB concentration versus time by the cell dry weight.

Analysis of Substrates and Products

MAA, MHB, glucose, and extracellular metabolites were analyzed by HPLC as described previously (Siedler et al., 2011). Glucose concentrations were in addition determined enzymatically by using the glucose Gluc-DH FS* Kit according to the manufacturer's instructions (DiaSys, Holzheim, Germany).

RNA Preparation, cDNA Synthesis, and DNA Microarray Analysis

For RNA preparation, *E. coli* strains were harvested 10 min after resuspension in biotransformation buffer before the addition of MAA and 10 min after the addition of MAA. For cell harvest, 20 mL of the cultures were poured into precooled (−20°C) tubes containing 15 g of ice and centrifuged (3 min, 4,200*g*, 4°C). The cell pellets were frozen in liquid nitrogen and stored at −70°C until RNA isolation, as described previously (Polen et al., 2003). DNA microarrays for *E. coli* were obtained from Microarrays, Inc. (Huntsville, AL). The array design includes 9,308 longmer oligonucleotide (70 mer) probes, representing genomes of four *E. coli* strains and three plasmids (4,269 ORFs in K-12, 5,306 ORFs in O157:H7, 5,251 ORFs in O157:H7, 5,366 ORFs in CFT073, 3 genes in OSAK1, 10 genes in pO157_Sakai, 97 genes in pO157_EDL933). Some genes are represented by different gene-specific oligonucleotides (e.g., *guaD*). Only genes of *E. coli* K-12 were analyzed. We applied the available K-12 DNA microarrays since comparisons of the B and K-12 genome sequences and the annotated protein coding genes showed >99% sequence identity over ~92% of their genomes with a total of ~4,039 coding sequences in the genome of the common ancestor, of which 97.6% remain evident in K and 96.5% in B (Jeong et al., 2009; Studier et al., 2009). The comparisons of the responses to the addition of MAA of the two strains were performed in duplicate, while the analysis of the differences of the two strains was done from three independent biological replicates. The details for handling the microarrays, data processing and data analysis have been described elsewhere (Hanke et al., 2012). Lists of differentially expressed genes were obtained by filtering the data using the following criteria: (i) flags ≥0 (GenePix Pro 6.0); (ii) signal to noise ratio ≥3 for red (F635med/B635med, GenePixPro 6.0) or green (F532med/B532med, GenePixPro 6.0); and (iii) averaged mRNA level change of ≥2-fold (strain comparison, Table II) or ≥2.5-fold (influence of MAA, Table III) and *P*-values ≤0.05. Processed and normalized data, as well as experimental details according to the MIAME guidelines (Brazma et al., 2001), were stored in the in-house microarray database (Polen and Wendisch, 2004).

Results and Discussion

Influence on Global Gene Expression of NADPH-Dependent Whole-Cell Biotransformation by Resting Cells of *E. coli* Using Glucose as Reductant

In order to study the influence of an NADPH-dependent whole-cell biotransformation on global gene expression, we analyzed the reduction of MAA to MHB by resting cells of *E. coli* and its Δ*pfkA* mutant, both carrying plasmid pBTac-*Lbadh* encoding an alcohol dehydrogenase from *L. brevis*. Cells resuspended to $3\,g_{cdw}\,L^{-1}$ in a phosphate buffer (pH 6.5) containing 110 mM glucose were incubated at 37°C and 130 rpm for 10 min in a shake flask. Then biotransformation was started by the addition of 60 mM MAA. Directly before and 10 min after MAA addition samples were taken for RNA isolation. The resulting RNA preparations were then used for comparative DNA microarray analyses and the mRNA ratios (after vs. before MAA addition) were determined for both the reference strain and the Δ*pfkA* mutant. The number of detectable genes (signal to noise ratio ≥3 for red or green) were about 91% and together with the distribution in M/A plots indicate that basically RNA from resting cells at the early time point of the biotransformation can also be applied to global gene expression analysis as RNA from growing or early stationary cells (e.g., Neusser et al., 2010, and Fig. S2). Thus, DNA microarray experiments represent an efficient tool to analyze resting cells under biotransformation conditions with respect to global gene expression.

In both strains, less than 20 genes showed a ≥2.5-fold increased or decreased mRNA ratio (Table II). Most interesting was a set of four genes whose expression was elevated in both strains after the addition of MAA, but two- to fivefold more strongly in the Δ*pfkA* mutant: *soxS* (24.4 vs. 4.6), *yqhC* (mRNA ratio 7.9 vs. 3.7), *yqhD* (36.2 vs. 12.7), and *dkgA* (16.2 vs. 7.4).

The *soxS* gene encodes an AraC-type transcriptional regulator, which controls genes involved in the response to oxidative stress (Greenberg et al., 1990; Pomposiello et al., 2001; Tsaneva and Weiss, 1990). Under stress conditions,

Table II. Influence of NADPH-dependent reductive biotransformation of MAA to MHB with glucose as reductant on global gene expression in *E. coli* and its Δ*pfkA* mutant.

Locus tag	Gene	Annotation	mRNA ratio reference + MAA/−MAA	mRNA ratio Δ*pfkA* + MAA/−MAA
Regulation				
ECD_01489	*marR*	Transcriptional repressor of multiple antibiotic resistance	2.07*	2.63
ECD_02423	*iscR*	DNA-binding transcriptional repressor	1.67*	5.83
ECD_02467	*rpoE*	Sigma factor E (σ24)	3.56	1.36*
ECD_02883	*yqhC*	Transcriptional activator of *yqhD* and *dkgA*	3.70	7.89
ECD_03754	*glnL*	Sensory histidine kinase	−1.32*	−2.00*
ECD_03934	*soxS*	DNA-binding transcriptional dual regulator	4.59	24.38
Metabolism				
ECD_01236	*trpC*	Bifunctional indole-3-glycerol phosphate synthase	3.74	1.14*
ECD_02884	*yqhD*	NADP-dependent aldehyde reductase	12.70	36.24
ECD_02885	*dkgA*	2,5-Diketo-D-gluconate reductase A	7.36	16.18
ECD_03288	*gntK*	Gluconate kinase	4.40	2.74
ECD_03591	*tnaL*	Tryptophanase leader peptide	2.85	n.d.
ECD_03755	*glnA*	Glutamine synthetase	−1.32*	−3.33
Transport				
ECD_00778	*glnH*	Glutamine ABC transporter, periplasmic binding protein	−2.5	−2.94
ECD_02533	*proV*	Glycine betaine transporter subunit	2.47*	−1.35*
ECD_02534	*proW*	Glycine betaine transporter subunit	2.90	−1.18*
Stress response				
ECD_01323	*ydaQ*	Putative excisionase of Rac prophage	−2.86	1.16*
ECD_10012	*ybcC*	Predicted exonuclease of DLP12 prophage	2.54	−1.27*
ECD_02420	*iscA*	Iron–sulfur cluster assembly protein	2.05*	1.81*
ECD_02421	*iscU*	Scaffold protein	1.76*	3.14
ECD_02422	*iscS*	Cysteine desulfurase	2.24*	3.04
Hypothetical/predicted function				
ECD_01108	*ycfR*	Hypothetical protein	7.25	5.25
ECD_01025	*ycdR*	Predicted enzyme associated with biofilm formation	−2.56	1.06*

DNA microarray analysis was used to compare RNA isolated 10 min after MAA addition to resting cells with RNA isolated before MAA addition (mean values from two biological replicates). Genes showing a significantly (P-value ≤ 0.05) increased or decreased mRNA ratio (≥ 2.5-fold) in either comparison are listed. Genes and lower mRNA ratio values were included for operons and for comparison of the two strains (indicated by an asterisk). The genes were sorted into functional groups, within which they are ordered according to their locus tag. Annotations were taken from the NCBI genome database.

expression of *soxS* is activated by SoxR, a dimeric transcriptional regulator of the MerR family with two [2Fe-2S] clusters (Hidalgo et al., 1998). SoxR itself becomes activated by oxidation of the [2Fe-2S] cluster. Inactivation of oxidized SoxR occurs via NADPH-dependent reduction, which requires the *rseC* and *rsxABCDGE* gene products (Koo et al., 2003). The intrinsic instability of the SoxS protein allows the response to be turned off once SoxR is reduced (Griffith and Wolf, 2004). The SoxRS system has been intensively studied in *E. coli* and there are multiple ways to induce the regulon. Evidence has been provided that the NADPH availability plays a crucial role in the induction of the SoxRS response (Krapp et al., 2011; Liochev and Fridovich, 1992) and we recently used the SoxRS system for the development of a single-cell NADPH sensor (Siedler et al., 2014). In our biotransformation experiments, cells face a very high NADPH demand when MAA, the substrate for the *L. brevis* alcohol dehydrogenase, is present, causing a decrease of the NADPH/$NADP^+$ ratio (Table S1). The strong NADPH consumption by MAA reduction is likely to impede the NADPH-dependent reduction of oxidized SoxR, causing activation of *soxS* expression. The 5.3-fold higher *soxS* mRNA ratio in the Δ*pfkA* mutant compared to the reference strain (24.4 vs. 4.6) might reflect the stronger decrease of the NADPH/$NADP^+$ ratio upon substrate addition (Table S1). Whereas expression of *soxS* was increased in our experiments, experimentally confirmed SoxS target genes, like *zwf* encoding glucose 6-phosphate dehydrogenase, did not show increased mRNA levels. We assume that the non-induction of the SoxS target genes is a consequence of the experimental conditions hindering SoxS protein synthesis. As the biotransformation buffer did not contain any nitrogen and sulfur sources, de novo protein synthesis should be very restricted. This assumption was supported by analyzing the expression of the *eyfp* gene under the control of the *soxS* promoter using the plasmid pSenSox, which also encodes the *Lbadh* gene (Siedler et al., 2014). As shown in Figure S3, a strong increase of EYFP fluorescence was observed when MAA was added to cells incubated in rich 2xYT medium, whereas only a very low fluorescence increase was observed when MAA was added to cells incubated in biotransformation buffer.

The *yqhC* gene encodes a transcriptional regulator of the AraC family that was shown to activate transcription of *yqhD* and *dkgA*, which are located divergent to *yqhC* (Lee et al., 2010; Turner et al., 2011). The *yqhD* gene product functions as a broad-substrate range NADPH-dependent aldehyde reductase (Jarboe, 2011; Lee et al., 2010). The *dkgA* gene (previously

Table III. Selected genes of a genome-wide direct comparison of mRNA levels in the Δ*pfkA* mutant versus the reference strain during NADPH-dependent reductive biotransformation of MAA to MHB with glucose as reductant.

Locus tag	Gene	Annotation	mRNA ratio Δ*pfkA*/reference
Metabolism			
ECD_00681-84	*sdhCDAB*	Succinate dehydrogenase	3.04–15.46
ECD_02266, ECD_02950, ECD_03737	*fadB*, *fadH*, *fadI*	Fatty acid metabolism	3.71–13.37
ECD_03905-08	*malEF, malK-lamB-malM*	Maltose metabolism	3.31–6.78
ECD_01164	*dadA*	D-Amino acid dehydrogenase, small subunit	5.43
ECD_00115	*lpdA*	Dihydrolipoamide dehydrogenase	2.34
ECD_00112	*pdhR*	Transcriptional regulator of pyruvate dehydrogenase complex genes	−2.56
ECD_03637	*rbsB*	Ribose transporter/kinase	−2.94
ECD_03028	*mtr*	Tryptophan transporter	−7.14
ECD_01234-39	*trpLECDBA*	Tryptophan biosynthesis	−5.88 to −20
ECD_03592-93	*tnaAB*	Tryptophanase/L-cysteine desulfhydrase, tryptophan transporter	−4.35 to −50
ECD_03801	*pfkA*	6-Phosphofructokinase	−20
Osmotic stress response			
ECD_00268-70	*betIB*, *betT*	Transcriptional regulator, betaine aldehyde dehydrogenase, choline transporter	3.78–7.44
Respiration and oxidative stress			
ECD_03934	*soxS*	DNA-binding transcriptional regulator	6.25
ECD_00382-83	*cyoBA*	Subunit I and II of cytochrome bo_3 ubiquinol oxidase	2.80–5.26
ECD_02423	*iscR*	Transcriptional repressor of genes involved in Fe-S cluster assembly	2.49
ECD_02464-65	*rseBC*	Periplasmic negative regulator RseB of sigma factor E, RseC protein involved in reduction of the SoxR iron–sulfur cluster	−2.22
ECD_00692	*cydA*	Cytochrome *bd* terminal oxidase, SU I	−3.70
ECD_00693	*cydB*	Cytochrome *bd* terminal oxidase, SU II	−2.63
Other functions			
		30 Ribosomal proteins	3.19–15.97
ECD_03847	*sthA*	Soluble transhydrogenase	3.05
ECD_01067-74	*flgM*, *flgA*, *flgBCDEFG*	Flagellar genes	2.44–3.21

Genes showing a ≥2-fold increased or decreased mRNA ratio are listed (*P*-value of ≤0.05). Genes highlighted in light gray are known to be repressed by the phosphorylated response regulator ArcA of the ArcAB two-component system and the genes highlighted in dark gray are known to be activated by phosphorylated ArcA. The data shown represent mean values from three biological replicates. The genes were grouped into different functional categories, within which they were ordered according to their mRNA ratios except in the case of operons, which were ordered according to their locus tag. A list of all genes with a ≥2-fold increased or decreased mRNA ratio is given in Table S2.

named *yqhE*) was originally characterized as an NADPH-dependent 2,5-diketo-D-gluconate reductase (Yum et al., 1999) and later shown to reduce also ethyl acetoacetate, other 2-keto esters, furfural, methylglyoxal, glyceraldehyde, benzaldehyde, valeraldehyde, and D-threose (Habrych et al., 2002; Jeudy et al., 2006). The mechanism of activation of YqhC is not yet known. Although it is tempting to speculate that substrates of YqhD or DkgA could serve as co-activators for YqhC, experimental data are not available yet.

Transcriptome Comparison of an *E. coli* Δ*pfkA* Mutant and Its Parent During MAA Reduction by Resting Cells

In order to detect the influence of a *pfkA* deletion on global gene expression during reductive biotransformation, a direct transcriptome comparison of the Δ*pfkA* mutant and the reference strain was performed with the RNA samples isolated 10 min after MAA addition, which were also used for the comparison with the RNA samples isolated before MAA addition (see above). In this series of DNA microarray experiments, 85 genes with ≥2-fold increased mRNA levels and 49 genes with ≥2-fold decreased mRNA levels were observed in the Δ*pfkA* mutant. A selection of these genes is shown in Table III and the complete list in Table S2.

It is evident that the absence of phosphofructokinase A and the resulting change in glucose catabolism has diverse effects on the expression of genes involved in respiration, metabolism, regulation and signal transduction, transport, motility, stress responses, transcription, and translation. For example, elevated mRNA levels were observed in the Δ*pfkA* mutant for the genes encoding succinate dehydrogenase (*sdhCDAB*, mRNA ratios 3.0–15.5), for genes involved in fatty acid metabolism (*fadB*, *fadH*, *fadhI*, mRNA ratios 3.7–13.4), as well as for genes involved in stress responses, such as osmotic stress (*betBIT*, mRNA ratios 3.8–7.4) and oxidative stress (*soxS*, mRNA ratio 6.3; *iscR*, mRNA ratio 2.5). The sixfold higher *soxS* mRNA level in the Δ*pfkA* mutant confirmed the microarray results described above (Table II). The *rseC* gene (ECD_02464, mRNA ratio 0.5), encoding a protein involved in the NADPH-dependent reduction of the iron sulfur cluster of SoxR, displayed a decreased mRNA level in the Δ*pfkA* mutant. In concert with a lowered NADPH availability after the addition

of MAA (Table S1), reduced *rseC* expression might reinforce a shift of SoxR to the active oxidized state and thus increased expression of *soxS*. The *sthA* gene encoding a soluble transhydrogenase displayed a more than threefold increased mRNA level in the Δ*pfkA* mutant, indicating an imbalanced redox ratio of the NAD(P)H pools. This result is coherent with a high flux through SthA transhydrogenase in the Δ*pfkA* mutant under growth conditions (Siedler et al., 2012).

Thirty genes encoding ribosomal proteins showed 3- to 16-fold increased mRNA levels in the Δ*pfkA* mutant. Literature data on the interdependence of cell growth, gene expression, and ribosome availability show that the growth rate and the RNA/protein ratio correlate (Scott et al., 2010), and in a Δ*pfkA* mutant of *E. coli* growth and ribosome content were reduced (Cardinale et al., 2013). However, the underlying studies were performed with growing cells and therefore may not be simply transferable to the resting cells used in the biotransformation. In the comparison made here, the differences in the expression of ribosomal protein genes might be due to an increased activity of the ArcAB two-component system in the reference strain, causing a repression of these genes (see below).

The most strongly decreased mRNA levels in the Δ*pfkA* mutant besides *pfkA* itself were found for genes involved in tryptophan biosynthesis, possibly due to the higher carbon flux through the PPP resulting in an increased availability of tryptophan precursors and possibly an increased tryptophan synthesis. High tryptophan levels are known to cause repression of the tryptophan biosynthesis operon *trpEDCBA* by activation of the repressor TrpR (Klig et al., 1988; Sarsero et al., 1991).

Transcriptional network analysis was used to identify relevant transcriptional regulators of the 134 genes with an altered mRNA level in the Δ*pfkA* mutant (Table S2). Target genes were found within these 134 genes for 36 out of 144 transcriptional regulators (Table S3). Besides the SoxR and TrpR regulons discussed above, another particularly interesting regulon was that of the response regulator ArcA, some members of which are highlighted in Table III (see also Table S4). The ArcAB two-component system was reported to sense microaerobic conditions by an increased QH_2/Q ratio (Cho et al., 2006; Georgellis et al., 2001; Green and Paget, 2004; Lamark et al., 1996; Liu and De Wulf, 2004; Malpica et al., 2006; Park et al., 2013; Spiro and Guest, 1991). This ratio is positively correlated with the NADH/NAD^+ ratio via the NADH dehydrogenases. The Δ*pfkA* mutant showed an 8% lower NADH/NAD^+ ratio than the reference strain after 30 min of biotransformation in shake flasks and after 120 min the difference was as much as 29% (Table S1). This suggests that the QH_2/Q ratio of the reference strain is higher than that of the Δ*pfkA* mutant, which in turn would suggest a higher ArcAB activity in the reference strain. The increased mRNA level of *cyoAB* encoding subunits of cytochrome bo_3 oxidase and the decreased mRNA level of *cydA* coding for a subunit of cytochrome *bd* oxidase in the Δ*pfkA* mutant is in agreement with these suggestions, as the *cyo* genes are repressed by ArcA and the *cyd* genes are activated by ArcA (Table S4).

The Crp regulon overlaps with the ArcA regulon, and transcriptional network analysis also revealed 34 Crp target genes (Table S3). Nineteen of them are known to be activated by Crp and showed elevated mRNA levels in the Δ*pfkA* mutant, suggesting an increased Crp activity due to an elevated cAMP level (Table S5). However, 13 target genes also known to be activated by Crp displayed decreased mRNA levels in the Δ*pfkA* mutant (Table S5) indicating a more complex regulation of these genes.

Comparison of Biotransformations Under Defined Anaerobic and Aerobic Conditions

The question of the causes and effects of a higher NADH/NAD^+ ratio and a stronger activity of the ArcAB two-component system in the reference strain during reductive biotransformation in shake flasks prompted us to analyze MAA reduction to MHB under controlled oxygen supply in a DASGIP bioreactor (Table IV). Under anaerobic conditions, the Δ*pfkA* mutant and the reference strain showed comparable MHB production rates (7.4 $mmol\,h^{-1}\,g_{cdw}{}^{-1}$), whereas the glucose uptake rate of the Δ*pfkA* deletion mutant (2.4 $mmol\,h^{-1}\,g_{cdw}{}^{-1}$) was much lower than that of the reference strain (3.5 $mmol\,h^{-1}\,g_{cdw}{}^{-1}$). This resulted in a 48% higher molar MHB/glucose yield of the mutant compared to the reference strain. Despite the reduced glucose uptake rate of the Δ*pfkA* mutant, its CO_2 transfer rate was comparable to that of the reference strain (Fig. S4).

Table IV. MHB production rate, glucose uptake rate, and molar MHB per glucose yield under different oxygen regimes for whole-cell reductive biotransformation of MAA to MHB with glucose as reductant.

E. coli strain	Condition	MHB production rate ($mmol\,h^{-1}\,g_{cdw}{}^{-1}$)	Glucose uptake rate ($mmol\,h^{-1}\,g_{cdw}{}^{-1}$)	Yield ($mol_{MHB}\,mol_{Glucose}{}^{-1}$)
Reference	Anaerobic	7.4 ± 0.1	3.5 ± 0.1	2.1 ± 0.1
Δ*pfkA*	Anaerobic	7.4 ± 0.2	2.4 ± 0.2	3.1 ± 0.2
Reference	Aerobic	12.8 ± 0.1	3.81 ± 0.1	3.4 ± 0.1
Δ*pfkA*	Aerobic	11.0 ± 0.3	2.3 ± 0.2	4.8 ± 0.1
Reference	Shake flask[a]	8.6 ± 0.1	3.4 ± 0.2	2.5 ± 0.2
Δ*pfkA*	Shake flask[a]	9.1 ± 0.3	1.8 ± 0.1	4.8 ± 0.1

Mean values from two independent experiments are shown for the *E. coli* reference strain and the Δ*pfkA* mutant.
[a]Values taken from Siedler et al. (2011).

Table V. Formation of fermentation products, by-products, and carbon dioxide, uptake of glucose and carbon balances of the *E. coli* BL21(DE3) reference strain and the Δ*pfkA* mutant during aerobic (30% DO) and anaerobic biotransformations.

Strain		Fermentation products or by-products						
		Acetate	Formate	Lactate	Succinate	CO_2	Glucose uptake	Balance
E. coli	Condition	($mmol\,h^{-1}\,g_{cdw}^{-1}$)				($mmol\,h^{-1}\,g_{cdw}^{-1}$)		(% C)
Reference	Anaerobic	3.3 ± 0.1	3.1 ± 0.3	2.6 ± 0.5	0.5 ± 0.001	2.8 ± 0.1	3.5 ± 0.1	106
Δ*pfkA*	Anaerobic	3.2 ± 0.1	3.1 ± 0.3	0.3 ± 0.01	0.4 ± 0.04	2.7 ± 0.2	2.4 ± 0.2	102
Reference	Aerobic	[a]	0	0	0	21.7 ± 0.2	3.8 ± 0.1	95
Δ*pfkA*	Aerobic	0	0	0	0	13.8 ± 0.3	2.3 ± 0.2	100

Mean values from two independent experiments are shown.
[a]Acetate was formed during the adaptation phase of the process and later consumed (*cf.* Fig. S5).

Formation of the mixed acid fermentation products acetate, formate, and succinate by the Δ*pfkA* mutant and the reference strain was similar, but lactate formation by the Δ*pfkA* mutant was reduced by almost 90% (Table V). The latter result can be explained by the fact that less NADH is synthesized in the *pfkA* mutant due to the altered glucose metabolism and additionally part of NADH might be used to reduce $NADP^+$ via transhydrogenase, as there is a strong NADPH demand for the biotransformation. The carbon balances were roughly closed for both strains under anaerobic conditions (Table V).

Under aerobic conditions (constant 15% DO), the MHB production rates of the reference strain (12.8 $mmol\,h^{-1}\,g_{cdw}^{-1}$) and of the Δ*pfkA* mutant (11.0 $mmol\,h^{-1}\,g_{cdw}^{-1}$) were 73% and 49% higher, respectively, than the rates observed under anaerobic conditions (Table IV). Again, the glucose uptake rate of the *pfkA* mutant (2.3 $mmol\,h^{-1}\,g_{cdw}^{-1}$) was significantly lower than that of the reference strain (3.8 $mmol\,h^{-1}\,g_{cdw}^{-1}$), resulting in a 41% increased molar MHB/glucose yield. To ensure steady-state aerobic conditions in the bioreactor, cells were first incubated for 30 min in the absence of the substrate MAA. During this adaptation time, no significant differences were observed either for the oxygen transfer rates (OTR) or for the carbon dioxide transfer rates (CTR) of the reference strain and the Δ*pfkA* mutant (Fig. 2). The similar OTR values might be explained by a high flux through the transhydrogenase SthA in the Δ*pfkA* mutant (Siedler et al., 2012), resulting in the conversion of NADPH generated in the cyclized PPP to NADH, which then drives respiration. After starting the biotransformation by the addition of MAA to the cell suspensions, both the OTR and the CTR markedly increased in the reference strain and later decreased again (Fig. 2). In contrast, the OTR of the Δ*pfkA* mutant rapidly dropped to zero and the CTR remained at the level observed immediately before MAA addition (Fig. 2). The strongly decreased respiration of the Δ*pfkA* mutant can be partially explained by the fact that in the presence of MAA the NADPH generated in the cyclized PPP is almost exclusively used by the *L. brevis* ADH (about 20 U mg protein^{-1}) for MAA reduction to MHB and is no longer available for NADH generation by the soluble transhydrogenase SthA. Most likely, the soluble transhydrogenase SthA cannot compete favorably with the overproduced Adh (17–28 $U\,mg^{-1}$; Siedler et al., 2011), even when *sthA* transcription is raised threefold. In fact, cell extracts of *E. coli* JM109 cultivated in rich SOB medium were reported to lack measurable SthA activity (detection limit approximately 0.001 $U\,mg^{-1}$) and only overexpression of *sthA* on a high-copy-number vector led to a high activity of 2.9 $U\,mg^{-1}$ (Boonstra et al., 1999).

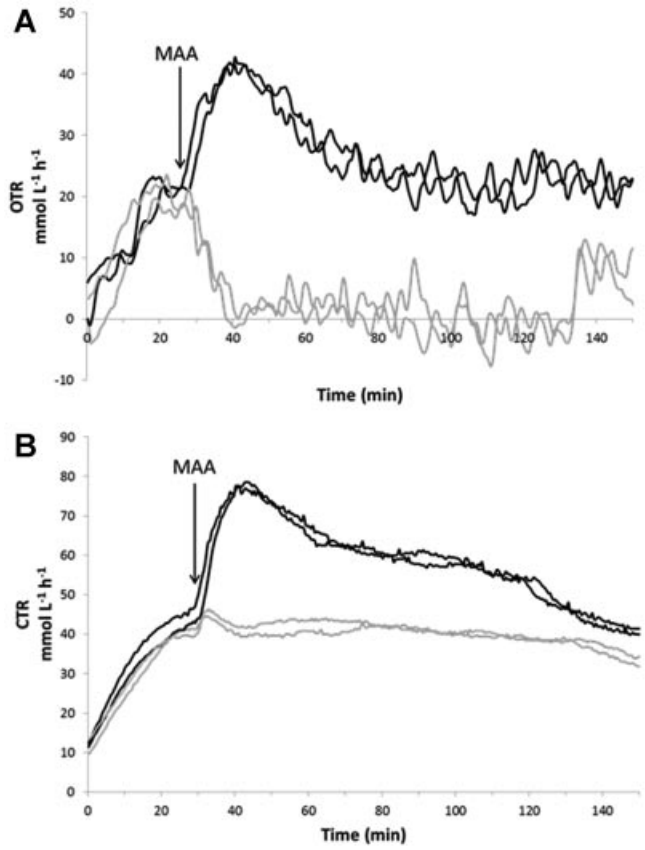

Figure 2. Oxygen transfer rates (OTR), (**A**) and CO_2 transfer rates (CTR), (**B**) during reductive biotransformation of MAA to MHB by the reference strain (black) and the Δ*pfkA* mutant (gray). The strains were incubated in buffer with glucose as reductant in a bioreactor and constantly supplied with 30% DO. After adaptation of the process and constant DO conditions, MAA was added as indicated by the arrow. Two biological replicates for each strain are shown.

The explanation given above was supported by the observation that the OTR of the Δ*pfkA* mutant increased again when MAA was completely reduced to MHB about 100 min after MAA addition (Fig. 2).

As the Δ*pfkA* mutant can still form NADH directly via glyceraldehyde 3-phosphate dehydrogenase, pyruvate dehydrogenase, or 2-oxoglutarate dehydrogenase, the OTR drop to zero after MAA addition indicates that either the flux through these reactions is rather low or that the NADH generated in these reactions is used by the membrane-bound transhydrogenase PntAB for proton-motive force-driven reduction of $NADP^+$. However, the latter reaction can also occur in the reference strain and therefore the differences in OTR after MAA addition between the Δ*pfkA* mutant and the reference strain must have other causes. A likely explanation is offered by the observation that the reference strain, but not the Δ*pfkA* mutant, accumulated acetate during the 30 min adaptation period before the addition of MAA. This acetate was consumed by the reference strain in the first 30 min after MAA addition (Fig. S5) and probably contributes to the increased OTR in this period. In particular, the succinate dehydrogenase and malate: ubiquinone oxidoreductase reactions, which form ubiquinol rather than NADH, might be the drivers of the OTR increase. Acetate oxidation by the reference strain can also explain the increased CTR observed after MAA addition.

When comparing the MHB production rates and MHB/glucose yield under aerobic and anaerobic conditions, it is evident that oxygen has a positive influence on both parameters and in both the reference strain and the Δ*pfkA* mutant. In the case of the reference strain, the yield under aerobic conditions in the bioreactor (3.4 mol/mol) is 62% higher than under anaerobic conditions and still 36% higher than under shake flask conditions, indicating oxygen-limiting conditions in the latter. In the case of the Δ*pfkA* mutant, the yield under aerobic conditions in the bioreactor (4.8 mol/mol) was 55% higher than under anaerobic conditions and identical to the yield observed in shake flasks. When using Δ*pfkA* mutants with a partially cyclized PPP for NADPH-dependent biotransformations, the demand for oxygen is much lower than that of the reference strain. Apart from supplying more NADPH for biotransformations, the application of such mutants requires less oxygenation and thus is less cost-intensive. More comprehensive knowledge of the consequences of reductive whole-cell biotransformations on metabolism and regulation is beneficial to support the optimization of production organisms and processes.

This work was supported by the Ministry of Innovation, Science, Research and Technology of North Rhine-Westphalia (Bio.NRW, Technology Platform Biocatalysis, RedoxCell support code: W0805wb001b).

References

Akinterinwa O, Cirino PC. 2011. Anaerobic obligatory xylitol production in *Escherichia coli* strains devoid of native fermentation pathways. Appl Environ Microbiol 77(2):706–709.

Boonstra B, French CE, Wainwright I, Bruce NC. 1999. The *udhA* gene of *Escherichia coli* encodes a soluble pyridine nucleotide transhydrogenase. J Bacteriol 181(3):1030–1034.

Brazma A, Hingamp P, Quackenbush J, Sherlock G, Spellman P, Stoeckert C, Aach J, Ansorge W, Ball CA, Causton HC, Gaasterland T, Glenisson P, Holstege FC, Kim IF, Markowitz V, Matese JC, Parkinson H, Robinson A, Sarkans U, Schulze-Kremer S, Stewart J, Taylor R, Vilo J, Vingron M. 2001. Minimum information about a microarray experiment (MIAME)-toward standards for microarray data. Nat Genet 29(4):365–371.

Cardinale S, Joachimiak MP, Arkin AP. 2013. Effects of genetic variation on the *E. coli* host-circuit interface. Cell Rep 4:231–237.

Chin JW, Cirino PC. 2011. Improved NADPH supply for xylitol production by engineered *Escherichia coli* with glycolytic mutations. Biotechnol Prog 27(2):333–341.

Cho BK, Knight EM, Palsson BO. 2006. Transcriptional regulation of the *fad* regulon genes of *Escherichia coli* by ArcA. Microbiology 152(Pt 8):2207–2219.

Ernst M, Kaup B, Müller M, Bringer-Meyer S, Sahm H. 2005. Enantioselective reduction of carbonyl compounds by whole-cell biotransformation, combining a formate dehydrogenase and a (*R*)-specific alcohol dehydrogenase. Appl Microbiol Biotechnol 66(6):629–634.

Georgellis D, Kwon O, Lin EC. 2001. Quinones as the redox signal for the Arc two-component system of bacteria. Science 292:2314–2316.

Goldberg K, Schroer K, Lütz S, Liese A. 2007. Biocatalytic ketone reduction—A powerful tool for the production of chiral alcohols-part II: Whole-cell reductions. Appl Microbiol Biotechnol 76(2):249–255.

Greenberg JT, Monach P, Chou JH, Josephy PD, Demple B. 1990. Positive control of a global antioxidant defense regulon activated by superoxide-generating agents in *Escherichia coli*. Proc Natl Acad Sci USA 87(16):6181–6185.

Green J, Paget MS. 2004. Bacterial redox sensors. Nat Rev Microbiol 2(12):954–966.

Griffith KL, Wolf RE Jr. 2004. Genetic evidence for pre-recruitment as the mechanism of transcription activation by SoxS of *Escherichia coli*: The dominance of DNA binding mutations of SoxS. J Mol Biol 344(1):1–10.

Habrych M, Rodriguez S, Stewart JD. 2002. Purification and identification of an *Escherichia coli* beta-keto ester reductase as 2,5-diketo-D-gluconate reductase YqhE. Biotechnol Prog 18(2):257–261.

Hanahan D, Jessee J, Bloom FR. 1991. Plasmid transformation of *Escherichia coli* and other bacteria. Methods Enzymol 204:63–113.

Hanke T, Richhardt J, Polen T, Sahm H, Bringer S, Bott M. 2012. Influence of oxygen limitation, absence of the cytochrome bc_1 complex and low pH on global gene expression in *Gluconobacter oxydans* 621H using DNA microarray technology. J Biotechnol 157(3):359–372.

Hidalgo E, Leautaud V, Demple B. 1998. The redox-regulated SoxR protein acts from a single DNA site as a repressor and an allosteric activator. EMBO J 17(9):2629–2636.

Ishige T, Honda K, Shimizu S. 2005. Whole organism biocatalysis. Curr Opin Chem Biol 9(2):174–180.

Jackson JB. 2003. Proton translocation by transhydrogenase. FEBS Lett 545(1):18–24.

Jarboe LR. 2011. YqhD: A broad-substrate range aldehyde reductase with various applications in production of biorenewable fuels and chemicals. Appl Microbiol Biotechnol 89(2):249–257.

Jeong H, Barbe V, Lee CH, Vallenet D, Yu DS, Choi SH, Couloux A, Lee SW, Yoon SH, Cattolico L, Hur CG, Park HS, Segurens B, Kim SC, Oh TK, Lenski RE, Studier FW, Daegelen P, Kim JF. 2009. Genome sequences of *Escherichia coli* B strains REL606 and BL21(DE3). J Mol Biol 394(4):644–652.

Jeudy S, Monchois V, Maza C, Claverie JM, Abergel C. 2006. Crystal structure of *Escherichia coli* DkgA, a broad-specificity aldo-keto reductase. Proteins 62(1):302–307.

Klig LS, Carey J, Yanofsky C. 1988. *trp* repressor interactions with the *trp aroH* and *trpR* operators. Comparison of repressor binding *in vitro* and repression *in vivo*. J Mol Biol 202(4):769–777.

Koo MS, Lee JH, Rah SY, Yeo WS, Lee JW, Lee KL, Koh YS, Kang SO, Roe JH. 2003. A reducing system of the superoxide sensor SoxR in *Escherichia coli*. EMBO J 22(11):2614–2622.

Krapp AR, Humbert MV, Carrillo N. 2011. The *soxRS* response of *Escherichia coli* can be induced in the absence of oxidative stress and oxygen by modulation of NADPH content. Microbiology 157(Pt 4):957–965.

Lamark T, Rokenes TP, McDougall J, Strom AR. 1996. The complex *bet* promoters of *Escherichia coli*: Regulation by oxygen (ArcA), choline (BetI), and osmotic stress. J Bacteriol 178(6):1655–1662.

Lee C, Kim I, Lee J, Lee KL, Min B, Park C. 2010. Transcriptional activation of the aldehyde reductase YqhD by YqhC and its implication in glyoxal metabolism of *Escherichia coli* K-12. J Bacteriol 192(16):4205–4214.

Liochev SI, Fridovich I. 1992. Fumarase C, the stable fumarase of *Escherichia coli*, is controlled by the *soxRS* regulon. Proc Natl Acad Sci USA 89(13):5892–5896.

Liu X, De Wulf P. 2004. Probing the ArcA-P modulon of *Escherichia coli* by whole genome transcriptional analysis and sequence recognition profiling. J Biol Chem 279(13):12588–12597.

Malpica R, Sandoval GR, Rodriguez C, Franco B, Georgellis D. 2006. Signaling by the Arc two-component system provides a link between the redox state of the quinone pool and gene expression. Antioxid Redox Signal 8(5–6):781–795.

Neusser T, Polen T, Geissen R, Wagner R. 2010. Depletion of the non-coding regulatory 6S RNA in *E. coli* causes a surprising reduction in the expression of the translation machinery. BMC Genomics 11:165.

Park DM, Akhtar MS, Ansari AZ, Landick R, Kiley PJ. 2013. The bacterial response regulator ArcA uses a diverse binding site architecture to regulate carbon oxidation globally. PLoS Genet 9(10):e1003839.

Polen T, Rittmann D, Wendisch VF, Sahm H. 2003. DNA microarray analyses of the long-term adaptive response of *Escherichia coli* to acetate and propionate. Appl Environ Microbiol 69(3):1759–1774.

Polen T, Wendisch VF. 2004. Genomewide expression analysis in amino acid-producing bacteria using DNA microarrays. Appl Biochem Biotechnol 118(1–3):215–232.

Pomposiello PJ, Bennik MH, Demple B. 2001. Genome-wide transcriptional profiling of the *Escherichia coli* responses to superoxide stress and sodium salicylate. J Bacteriol 183(13):3890–3902.

Sarsero JP, Wookey PJ, Pittard AJ. 1991. Regulation of expression of the *Escherichia coli* K-12 *mtr* gene by TyrR protein and Trp repressor. J Bacteriol 173(13):4133–4143.

Sauer U, Canonaco F, Heri S, Perrenoud A, Fischer E. 2004. The soluble and membrane-bound transhydrogenases UdhA and PntAB have divergent functions in NADPH metabolism of *Escherichia coli*. J Biol Chem 279(8):6613–6619.

Scott M, Gunderson CW, Mateescu EM, Zhang Z, Hwa T. 2010. Interdependence of cell growth and gene expression: Origins and consequences. Science 330(6007):1099–1102.

Siedler S, Bringer S, Blank LM, Bott M. 2012. Engineering yield and rate of reductive biotransformation in *Escherichia coli* by partial cyclization of the pentose phosphate pathway and PTS-independent glucose transport. Appl Microbiol Biotechnol 93(4):1459–1467.

Siedler S, Bringer S, Bott M. 2011. Increased NADPH availability in *Escherichia coli*: Improvement of the product per glucose ratio in reductive whole-cell biotransformation. Appl Microbiol Biotechnol 92(5):929–937.

Siedler S, Schendzielorz G, Binder S, Eggeling L, Bringer S, Bott M. 2014. SoxR as a single-cell biosensor for NADPH-consuming enzymes in *Escherichia coli*. ACS Synth Biol 3(1):41–47.

Spiro S, Guest JR. 1991. Adaptive responses to oxygen limitation in *Escherichia coli*. Trends Biochem Sci 16(8):310–314.

Studier FW, Daegelen P, Lenski RE, Maslov S, Kim JF. 2009. Understanding the differences between genome sequences of *Escherichia coli* B strains REL606 and BL21(DE3) and comparison of the *E. coli* B and K-12 genomes. J Mol Biol 394(4):653–680.

Tan I. 2006. Applications of whole cell biotransformations for the production of chiral alcohols. PhD thesis, University of Bonn, Bonn, Germany.

Tsaneva IR, Weiss B. 1990. *soxR*, a locus governing a superoxide response regulon in *Escherichia coli* K-12. J Bacteriol 172(8):4197–4205.

Turner PC, Miller EN, Jarboe LR, Baggett CL, Shanmugam KT, Ingram LO. 2011. YqhC regulates transcription of the adjacent *Escherichia coli* genes *yqhD* and *dkgA* that are involved in furfural tolerance. J Ind Microbiol Biotechnol 38:431–439.

Yum DY, Lee BY, Pan JG. 1999. Identification of the *yqhE* and *yafB* genes encoding two 2,5-diketo-D-gluconate reductases in *Escherichia coli*. Appl Environ Microbiol 65(8):3341–3346.

Supporting Information

Additional supporting information may be found in the online version of this article at the publisher's web-site.